NEUROSCIENCE

Thirst-associated preoptic neurons encode an aversive motivational drive

William E. Allen,[1,2]* Laura A. DeNardo,[1]* Michael Z. Chen,[1]* Cindy D. Liu,[1,3] Kyle M. Loh,[4] Lief E. Fenno,[6] Charu Ramakrishnan,[5] Karl Deisseroth,[3,5,6]† Liqun Luo[1,3]†

Water deprivation produces a drive to seek and consume water. How neural activity creates this motivation remains poorly understood. We used activity-dependent genetic labeling to characterize neurons activated by water deprivation in the hypothalamic median preoptic nucleus (MnPO). Single-cell transcriptional profiling revealed that dehydration-activated MnPO neurons consist of a single excitatory cell type. After optogenetic activation of these neurons, mice drank water and performed an operant lever-pressing task for water reward with rates that scaled with stimulation frequency. This stimulation was aversive, and instrumentally pausing stimulation could reinforce lever-pressing. Activity of these neurons gradually decreased over the course of an operant session. Thus, the activity of dehydration-activated MnPO neurons establishes a scalable, persistent, and aversive internal state that dynamically controls thirst-motivated behavior.

To maintain homeostasis and ensure survival, physiological imbalances produce motivational drives: internal states that promote specific goal-directed behaviors and scale in duration, intensity, and valence (*1*–*5*). The classical "drive reduction" hypothesis posits that animals learn particular goal-directed behaviors to reduce the level of an aversive drive state (*1*, *2*, *6*). However, electrical stimulation experiments of putative hunger- and thirst-regulating nuclei indicate that motivational states increase the incentive value of stimuli or behaviors that led to reward (*4*, *7*, *8*). Recent experiments show that both positive and negative valence mechanisms appear to play a role in controlling feeding (*9*–*14*). By contrast, the neural mechanisms for the thirst motivational drive remain poorly understood.

The lamina terminalis of the hypothalamus has been implicated in water intake in mammals through lesion, optogenetic stimulation, and activity recording (*10*, *15*–*20*). In particular, the median preoptic nucleus (MnPO) integrates blood volume, osmolarity, and hormonal inputs from the circumventricular subfornical organ (SFO) and vascular organ of the lamina terminalis (OVLT) and broadcasts this information to multiple higher brain areas (*21*). This architecture makes MnPO potentially well suited to play a central role in producing thirst motivational drive. However, MnPO is a highly heterogeneous nucleus that regulates body temperature, sleep, cardiovascular function, and sodium excretion, in addition to thirst (*21*). It remains unknown how the activity of specific populations of neurons within this area regulates thirst motivation.

Water deprivation induces robust expression of *Fos* in several hypothalamic nuclei, including MnPO (*22*, *23*). To genetically access these cells, we used a new FosTRAP transgenic mouse line (*24*), *TRAP2*, in which *2A-iCreER^{T2}* was knocked into the *Fos* locus to create an in-frame fusion (*25*) (Fig. 1A). In *TRAP2;Ai14* double transgenic mice, neuronal activation results in the expression of CreER, which enters the nucleus in response to 4-hydroxytamoxifen (4-OHT) injection and causes recombination. This results in permanent expression of tdTomato (Cre reporter from *Ai14*) in active neurons (*24*–*26*) (Fig. 1B). Injecting 4-OHT into *TRAP2;Ai14* double transgenic mice produced many more tdTomato$^+$ neurons in the MnPO of mice deprived of water for 48 hours (Thirst-TRAP) compared with water-satiated controls (Homecage-TRAP) (Fig. 1, C, D, and F). We compared Thirst-TRAP with endogenous Fos protein expression after 48 hours of water deprivation. *TRAP2* labeling in MnPO had high efficiency (65% of Fos$^+$ cells were tdTomato$^+$) and specificity (96% of tdTomato$^+$ cells were Fos$^+$) (Fig. 1G). By contrast, few MnPO cells were double labeled with Fos after 48 hours of water deprivation in Homecage-TRAP mice (Fig. 1, C, E, and H). *TRAP2* also efficiently and specifically labeled cells in other hypothalamic nuclei that exhibited high Fos induction upon water deprivation (fig. S1).

MnPO also contains neurons involved in thermoregulation (*27*), and warm ambient temperature can cause robust MnPO Fos induction (*28*). After Thirst-TRAP, we challenged mice with a 37°C warm environment for 4 hours before sacrifice. Warmth-induced Fos was expressed in a spatially intermingled but nonoverlapping population compared with Thirst-TRAPed cells in MnPO (Fig. 1, C, E, and H).

Because MnPO and the surrounding medial preoptic area (MPOA) are highly molecularly heterogeneous, we applied single-cell RNA sequencing (*29*) to determine the full spectrum of TRAPed cell types. After Thirst-TRAP, we used fluorescence-activated cell sorting (FACS) to isolate tdTomato$^+$ neurons (~1% of viable cells) from microdissected preoptic hypothalamus and sequenced cDNA from each cell (Fig. 2A and fig. S2). Our microdissection included neurons in both target MnPO and the surrounding MPOA that appeared in both the Homecage- and Thirst-TRAP conditions. Dimensionality reduction and clustering of 348 single-cell transcriptomes that passed quality control revealed two clusters: a mostly inhibitory Cluster 1 (*Gad1*$^+$ encoding a biosynthetic enzyme for γ-aminobutyric acid) (N = 172 cells) and a predominantly excitatory Cluster 2 (*Slc17a6*$^+$ encoding a vesicular transporter for glutamate) (N = 176 cells) (Fig. 2, B to E, and table S1). Many of the top Cluster 1 genes were broadly expressed throughout the preoptic area (fig. S3A), and Cluster 1 exhibited substantial heterogeneity, including cells constitutively expressing the immediate early genes *Fos*, *Egr1*, and *Junb* (fig. S3B). By contrast, Cluster 2 was not clearly separable into subclusters and was characterized by high expression of specific receptors (e.g., the angiotensin II receptor *Agtr1a*), neuropeptides (e.g., *Nxph4* and *Adcyap1*), and transcription factors (e.g., *Etv1*) (Fig. 2C). Many Cluster 2 genes were highly expressed specifically in MnPO (fig. S3A), including *Nxph4*, *Adcyap1*, and *Bdnf*, previously described as enriched in warm-associated MnPO neurons (*27*), as well as *Agtr1a* specific to thirst-associated neurons. *Agtr1a*'s endogenous agonist, angiotensin II (ANG II), has long been implicated in regulating water balance within the lamina terminalis (*30*). These results suggest that Cluster 2 represents a distinct cell type of thirst-associated neurons within MnPO.

We validated this conclusion by examining the colocalization between marker genes and TRAPed preoptic neurons in situ. Using three-color amplified single-molecule fluorescence in situ hybridization (smFISH) (*31*), we simultaneously mapped the locations of *tdTomato*$^+$, *Gad1*$^+$ (inhibitory), and *Slc17a6*$^+$ (excitatory) neurons. Whereas 90% of *tdTomato*$^+$*Gad1*$^+$ neurons were outside MnPO, 91% of *tdTomato*$^+$*Slc17a6*$^+$ neurons were within MnPO (N = 2 mice, Fig. 2, F and G). Double smFISH between *tdTomato* and top Cluster 2 genes *Adcyap1*, *Agtr1a*, or *Nxph4* revealed that for each marker gene, *tdTomato*$^+$ cells represented less than a third of the total population of marker$^+$ cells within MnPO (double$^+$/marker$^+$ = 28, 31, and 28%, respectively). However, the vast majority of *tdTomato*$^+$ cells within MnPO coexpressed each marker gene (double$^+$/tdTomato$^+$ = 91, 89, and 98%, respectively, N = 3 mice; pie chart in Fig. 2, H to J). Thus, Thirst-TRAPed MnPO neurons appeared to constitute a single, molecularly defined cell type.

If these Thirst-TRAPed MnPO neurons encode thirst motivational drive, then their suppression in water-deprived animals should inhibit, while their reactivation in water-satiated animals should elicit, water consumption. We delivered virally encoded Cre-dependent iC++-2A-eYFP (enhanced

[1]Department of Biology, Stanford University, Stanford, CA 94305, USA. [2]Neurosciences Program, Stanford University, Stanford, CA 94305, USA. [3]Howard Hughes Medical Institute, Stanford University, Stanford, CA 94305, USA. [4]Institute for Stem Cell Biology and Regenerative Medicine, Stanford University, Stanford, CA 94305, USA. [5]Department of Bioengineering, Stanford University, Stanford, CA 94305, USA. [6]Department of Psychiatry and Behavioral Sciences, Stanford University, Stanford, CA 94305, USA.
*These authors contributed equally to this work. †Corresponding author. Email: deissero@stanford.edu (K.D.); lluo@stanford.edu (L.L.)

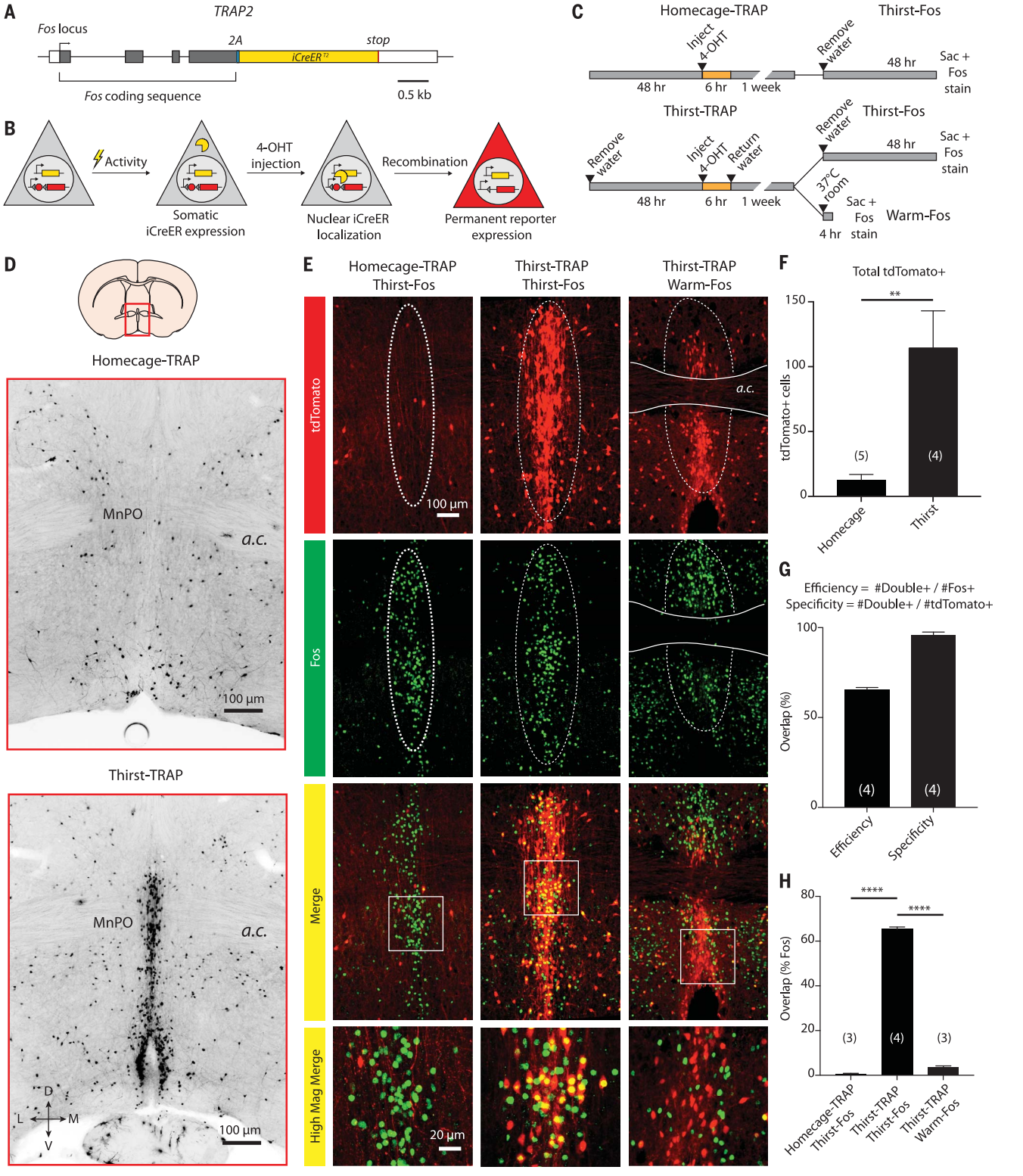

Fig. 1. TRAP2 efficiently and specifically labels dehydration-activated neurons in the median preoptic nucleus (MnPO). (**A** and **B**) *TRAP2* design and principle. (**C**) Experimental timelines to determine the efficiency and specificity of Thirst-TRAP, by comparing Thirst- or Homecage-TRAP tdTomato expression with Fos immunolabeling in response to 48 hours of water deprivation (Thirst-Fos) or 4 hours at 37°C (Warm-Fos). (**D**) tdTomato expression in MnPO after recombination of *TRAP2;Ai14* mice, under water-satiated (Homecage-TRAP) and 48-hours water-deprived (Thirst-TRAP) conditions. *a.c.*, anterior commissure; D, dorsal; V, ventral; M, medial; L, lateral. (**E**) Representative confocal images of tdTomato/Fos overlap for three conditions, as indicated above. (**F**) Quantification of total tdTomato induction in MnPO after recombination in Homecage- or Thirst-TRAP mice; *t* test. (**G**) Efficiency and specificity of MnPO Thirst-TRAP. (**H**) TRAP/Fos overlap ($Double^+/Fos^+$) for the three experimental groups, one-way ANOVA, Holm-Šidák correction. Numbers of mice quantified for each experiment are in parentheses. $^{**}P < 0.01$, $^{****}P < 1 \times 10^{-4}$. Data are presented as mean ± SEM.

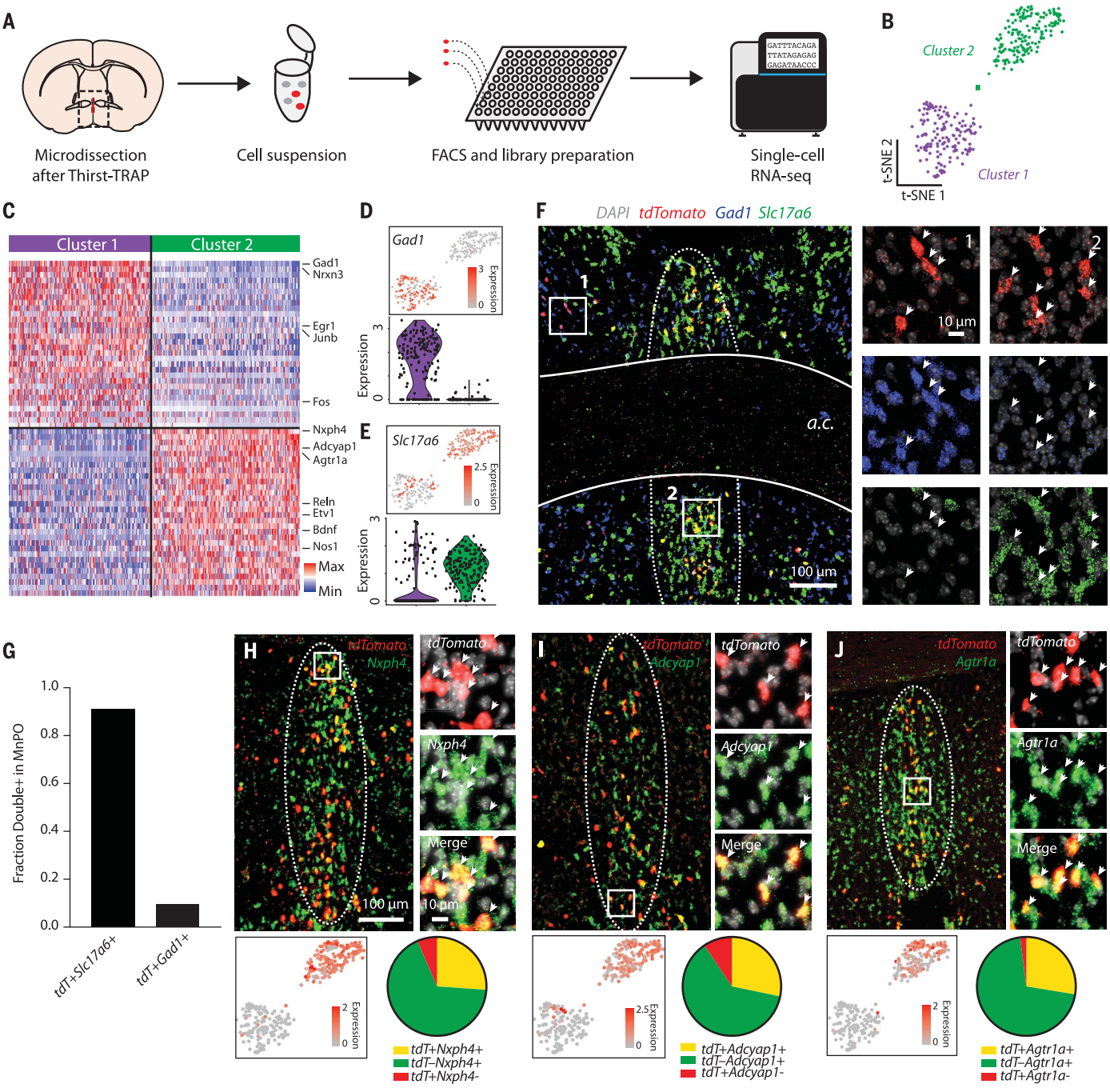

Fig. 2. Molecular identity of MnPO Thirst-TRAPed neurons. (**A**) Single-cell RNA-sequencing of MnPO Thirst-TRAPed neurons. Tissue containing MnPO of Thirst-TRAP mice is microdissected from live brain slices. Neurons are dissociated then FAC-sorted into 96-well plates. Single-cell cDNA libraries are prepared and sequenced together. (**B**) t-distributed stochastic neighbor embedding (t-SNE) representation of 348 transcriptomes showing two clusters. (**C**) Top 30 differentially expressed genes between the two clusters, per cluster, sorted by average difference in expression per cluster and *Z*-scored per gene. (**D** and **E**) (Top) t-SNE representation of cells colored by *Gad1* (D) or *Slc17a6* (E) expression. (Bottom) Expression of *Gad1* or *Slc17a6* in cells within Cluster 1 (purple) and Cluster 2 (green). Expression, log-normalized TPM (transcripts per million) values (see methods). (**F**) Three-color smFISH of *tdTomato* (red), *Gad1* (blue), and *Slc17a6* (green) in the MnPO (dotted oval) of a Thirst-TRAP mouse. (Left) Low-magnification view; two fields of view highlighted. (Right) High-magnification view of *tdTomato*$^+$ (red) cells outside MnPO (1) or within MnPO (2), along with *Gad1* and *Slc17a6* expression in the same cells, indicated with arrows. (**G**) Fraction of *tdTomato*$^+$*Slc17a6*$^+$ and *tdTomato*$^+$*Gad1*$^+$ neurons within MnPO, out of total *tdTomato*$^+$ cells. *N* = 2 mice. tdT, tdTomato. (**H** to **J**) Double smFISH of *tdTomato* and Cluster 2 markers, *Adcyap1*, *Agtr1a*, or *Nxph4*, in Thirst-TRAP mice. (Top left) Low-magnification view of marker and *tdTomato* with MnPO circled. (Top right) High-magnification view of *tdTomato* (red) and marker gene (green) expression. Arrows, double-labeled cells. (Bottom left) t-SNE representation of cells colored by expression of marker gene. (Bottom right) Fractional combinations of *tdTomato*$^+$ with each marker gene. *Adcyap1*: *N* = 276 total cells; *Agtr1a*: 396 total cells; *Nxph4*: 402 total cells, across *N* = 3 mice per marker gene.

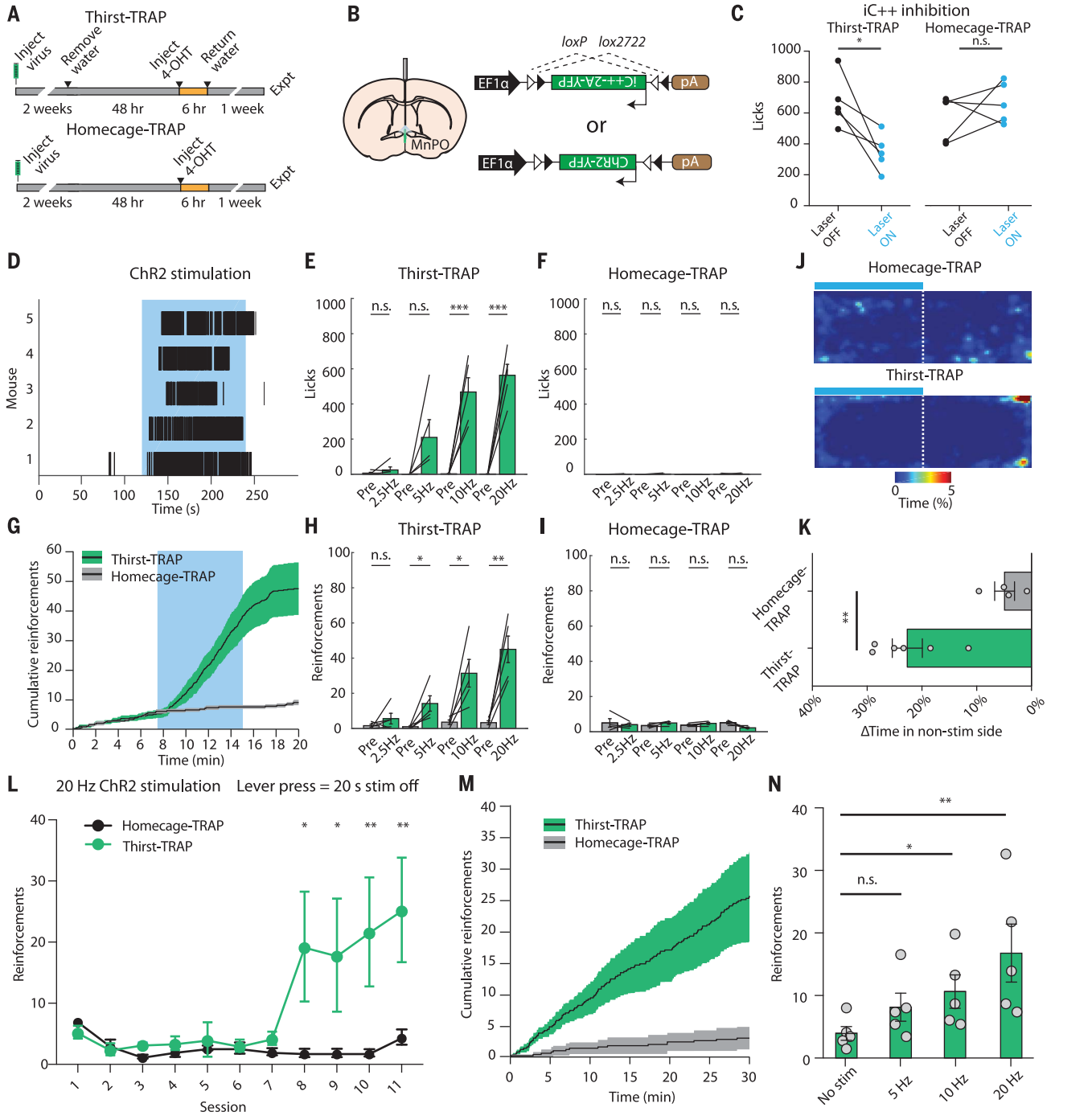

Fig. 3. Optogenetic activation of MnPO Thirst-TRAPed neurons induces a scalable, aversive thirst motivational state. (**A**) Experimental timeline for Thirst- and Homecage-TRAP to express a virally delivered effector. (**B**) (Left) Fiber-optic implant for illuminating MnPO. (Right) Viral constructs for Cre-inducible iC++ or ChR2 expression. (**C**) Total licks in water-restricted mice expressing iC++ in MnPO during 7.5-min laser-ON or laser-OFF session; paired *t* test. (**D**) Licking for water after 20-Hz stimulation (blue) of Thirst-TRAPed MnPO neurons expressing ChR2 in 5 water-satiated mice. (**E** and **F**) Total licks over 15-min prestimulation or stimulation period of *N* = 5 Thirst- (E) or Homecage- (F) TRAPed MnPO neurons at 2.5, 5, 10, and 20 Hz. (**G**) Cumulative reinforcements (water rewards) over 20 min, before, during (blue), and after 20-Hz stimulation, after training. *N* = 5 animals per group. (**H** and **I**) Total reinforcements within 15 min prestimulation or stimulation period of *N* = 5 water-satiated Thirst- (H) or Homecage- (I) TRAPed MnPO neurons at 2.5, 5, 10, and 20 Hz. (**J**) Real-time place preference (RTPP) to 20-Hz stimulation. (**K**) Aggregate RTPP data of difference in time on nonstimulated and stimulated sides; unpaired *t* test. (**L**) Reinforcements per 30-min session of mice learning to lever-press to receive a 20-s break in otherwise constant 20-Hz stimulation. Two-way ANOVA, Holm-Šidák correction. (**M**) Cumulative reinforcements over 30-min session. *N* = 5 Homecage- (gray) and *N* = 5 Thirst- (green) TRAP mice. (**N**) Total reinforcements within a 30-min session for Thirst-TRAP mice lever-pressing to turn off 0-, 5-, 10-, and 20-Hz MnPO stimulation; Kruskal-Wallis test, false discovery rate correction. **P* < 0.05, ***P* < 0.01, ****P* < 0.001. n.s., not significant. Data presented as mean ± SEM.

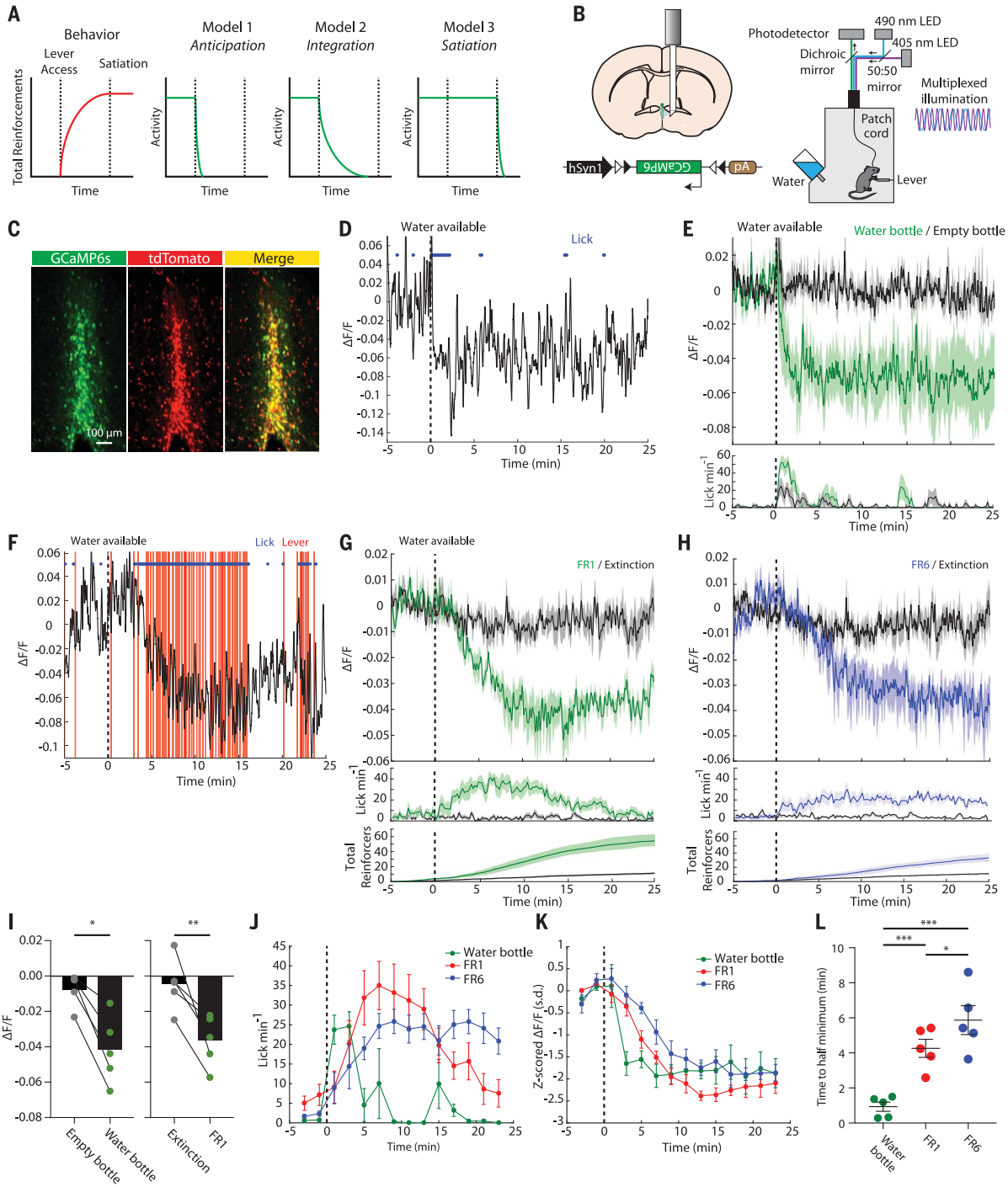

Fig. 4. MnPO thirst-associated neurons integrate water intake to control motivational drive. (**A**) Diagram of possible models relating MnPO activity dynamics and behavior. Behavioral trace represents idealized cumulative reinforcements as a mouse lever-presses for water. (**B**) Diagram of MnPO fiber photometry recordings with multiplexed Ca^{2+}-independent control (405 nm) and Ca^{2+}-dependent (490 nm) illumination. (**C**) Coexpression of GCaMP6s and tdTomato in Thirst-TRAP MnPO. (**D**) Single-trial MnPO activity dynamics upon drinking water in a water-restricted Thirst-TRAP mouse. (**E**) (Top) Average MnPO activity upon licking full (green) or empty (black) water bottle. (Bottom) Lick rate over time. $N = 5$ mice. (**F**) Single-trial MnPO activity dynamics during FR1 lever-pressing in water-restricted Thirst-TRAP mouse. (**G**) (Top) Average MnPO activity during task performance on a FR1 (green) or Extinction (black) schedule. (Extinction, no water delivered.) (Middle) Average licking behavior. (Bottom) Average cumulative reinforcements. $N = 5$ mice, averaged across $N = 3$ sessions per mouse. (**H**) Same as (G) but for mouse on FR6 schedule. (**I**) Quantification of average fluorescence during 5-min interval from $T = 10$ min to $T = 15$ min, after presentation of empty bottle or water bottle (E), or after onset of Extinction and FR1 schedule lever-pressing for water (G); paired t test. (**J** and **K**) Lick rate (J) or Z-scored MnPO activity (K) in 2-min bins for free drinking from water bottle (E), FR1 lever-pressing (G), and FR6 lever-pressing (H). (**L**) Time for activity to decrease to half minimal value for each mouse, based on sigmoid fit; two-way ANOVA, Benjamini-Hochberg correction. $^*P < 0.05$, $^{**}P < 0.01$, $^{***}P < 0.001$. n.s., not significant. Data presented as mean ± SEM.

yellow fluorescent protein) (*32*) (inhibitory opsin) or ChR2-eYFP (*33*) (excitatory opsin) to the MnPO of *TRAP2* mice and induced recombination after 48 hours of water deprivation, then delivered light to MnPO via a fiber implant (Fig. 3, A and B). Photoinhibition reduced water consumption in water-deprived Thirst-TRAPed mice but not water-deprived Homecage-TRAPed mice (Fig. 3C). By contrast, photoactivation of these neurons in water-satiated animals rapidly evoked water consumption, which terminated upon cessation of stimulation (Fig. 3D). The rate of water consumption scaled with the frequency of photoactivation [one-way analysis of variance (ANOVA) test for linear trend; $P < 0.001$] (Fig. 3E), whereas Homecage-TRAPed animals never drank water when photostimulated (Fig. 3F). Patch-clamp recordings in acute slices showed that ChR2-expressing Thirst-TRAPed MnPO neurons responded with high fidelity to photoactivation at 20 Hz (fig. S4, A and B), and optogenetic stimulation 90 min before sacrifice induced a drastic increase in Fos expression, specifically in Thirst-TRAPed MnPO (fig. S4, C and D). Stimulation of Thirst-TRAPed neurons in water-satiated mice did not cause undirected gnawing or licking behaviors (movie S1).

To determine whether activation of MnPO neurons simply causes water consumption or can motivate mice to perform an operant task for water, we water-restricted mice and trained them in a fixed ratio 1 (FR1) operant task, where each lever press leads to a unit of water reward. After training, mice were allowed free access to water and tested on the task while water-satiated. Photoactivation in water-satiated mice rapidly induced lever-pressing for water (Fig. 3G), the rate of which scaled with the frequency of stimulation (one-way ANOVA test for linear trend; $P < 0.001$) (Fig. 3H), whereas stimulation of Homecage-TRAPed neurons had no effect on behavior (Fig. 3I).

Classical theories of learning and motivation suggest that deviations from homeostatic set points are aversive and that animals perform motivated behaviors to reduce such aversive states (*1*, *2*, *4*). Consistent with this theory, real-time place preference assay revealed that mice vigorously avoided the photoactivation of Thirst-TRAPed but not Homecage-TRAPed neurons (Fig. 3, J and K). These data suggested that a reduction in the activity of Thirst-TRAPed MnPO neurons alone might be reinforcing. Indeed, mice learned to vigorously lever-press to turn off photoactivation of Thirst-TRAPed (but not Homecage-TRAPed) neurons over several 30-min sessions (Fig. 3L). Thirst-TRAPed mice would lever-press consistently for the whole duration of the session without any signs of satiation (Fig. 3M). The number of rewarded lever presses scaled with the frequency of stimulation (one-way ANOVA test for linear trend; $P < 0.05$) (Fig. 3N), suggesting that higher levels of Thirst-TRAPed MnPO neuron activity are more aversive and that the reduction in activity is more reinforcing.

The activity representing this aversive drive state must interface with other brain systems to produce coordinated goal-directed behavior. We found prominent axonal projections to several other subcortical areas, including lateral hypothalamus (LH), paraventricular hypothalamus (PVH), paraventricular thalamus (PVT), and supraoptic nucleus (SON) (fig. S5A). Optogenetic stimulation of MnPO increased the number of Fos^+ cells in PVT, PVH, and SON of Thirst-TRAPed mice relative to Homecage-TRAPed mice (fig. S5, B to D). Stimulation of ChR2-expressing Thirst-TRAPed MnPO neuron axon terminals in PVH, PVT, and LH all produced both water-drinking and FR1 lever-pressing in water-satiated mice (fig. S5, E to G). Even though individual MnPO neurons displayed limited collateralization (fig. S6), we cannot rule out the possibility that some of these effects were caused by back-propagating action potentials spreading from the stimulated area to other brain areas via collaterals. Finally, Cre-dependent transsynaptic rabies tracing from Thirst-TRAPed MnPO neurons revealed inputs from PVH, PVT, and thirst-related hypothalamic nuclei such as SFO and SON, as well as from the central amygdala (CeA) and parabrachial nucleus (PBN), which could relay other forms of sensory, valence, or satiety information (*34*, *35*) (fig. S7).

Finally, we investigated the in vivo dynamics of Thirst-TRAPed MnPO neurons during thirst-motivated behaviors. MnPO neurons respond to changes in blood osmolarity and circulating ANG II concentration, presumably via inputs from OVLT and SFO (*36*, *37*). MnPO neuron activity is presumed to decrease upon water intake but could potentially exhibit one of the following patterns (Fig. 4A). First, the activity decrease could be purely anticipatory: When animals sense the access to water, their MnPO activity immediately decreases. Second, these neurons could integrate water consumption over time. Third, these neurons could remain active and continue to drive behavior until a satiety signal is engaged that shuts off MnPO activity.

We expressed Cre-dependent GCaMP6 (*38*) in Thirst-TRAPed MnPO neurons and used fiber photometry to record changes in their activity during behavior (*39*) (Fig. 4, B and C). Free water consumption by thirsty mice rapidly decreased MnPO neuronal activity within ~1 min, similar to that of SFO^{Nos1} (*20*) neurons, with the decrease coinciding with the period spent licking for water (Fig. 4, D and E). Mice licking an empty bottle had no decrease in activity (Fig. 4, E and I). MnPO neurons also increased activity in response to 3 M saline injection and had no response to isotonic phosphate-buffered saline injection (fig. S8). However, because thirsty mice rapidly consume freely available water, it was difficult to discriminate between the various models relating MnPO activity to motivated behavior.

To reduce the rate of water consumption, we trained these mice on an FR1 operant task and recorded activity during task performance while the mice were water restricted. Lever-pressing for water resulted in a gradual decrease in MnPO activity over many minutes, much more slowly than during free drinking (Fig. 4G). The time when activity reached a minimum coincided with a decrease in the rate of licking and lever-pressing (Fig. 4G). When mice were put on an extinction schedule, with no water delivered for lever-pressing, there was no decrease in activity (Fig. 4, G and I). Control mice expressing YFP had no change in fluorescence during any behavior (fig. S9). We measured how quickly Thirst-TRAPed MnPO neuron activity decreased in an even slower FR6 task, where six lever presses yielded a unit of water. In this condition, the rate of reinforcements was lower than for FR1, as was the rate of decrease of MnPO activity over time (Fig. 4, H and J). Directly comparing the rates of licking over time between free access to water, FR1, and FR6, we found that mice tended to lick for progressively longer across these conditions (Fig. 4J), and activity correspondingly decreased more slowly as mice received water at a slower rate (Fig. 4, K and L). This slow time course of activity decrease, which correlated with progressive water intake, is inconsistent with the anticipation and satiation models; instead, MnPO neuron activity appears to integrate water intake over time.

Genetic access of activated neurons has emerged as an important tool to dissect neural circuit function (*40*). Using *TRAP2* (*25*), we show that the physiological imbalance following water deprivation produces a motivational drive encoded in the activity of a molecularly defined neuronal type within hypothalamic MnPO. This drive is aversive, scales with the activation frequency of thirst-associated MnPO neurons, and persists in driving behavior over long periods of time. The real-time reduction in activity of these neurons is reinforcing and, as such, is capable of conditioning instrumental behavior. The activity of these neurons integrates the recent history of water intake to adaptively regulate goal-directed behavior. When thirsty, animals perform actions that lead to water consumption, which reduces the aversive MnPO activity by some amount. These actions are repeated until enough water is consumed that the level of aversion ceases to evoke behavior. In doing so, an association is formed between particular actions and reduction of an aversive state, which would contribute to making those actions more likely to be repeated when the animal is thirsty again in the future. Together, our results suggest a mechanism for the implementation of thirst motivational drive in MnPO neurons that resembles the classical drive-reduction hypothesis (*1*, *2*, *4*). MnPO thirst neurons are connected to a variety of other brain regions (figs. S5 to S7) that could translate thirst drive into specific goal-directed actions. The extent to which thirst-motivated behaviors arise from negative-valence drive reduction mechanisms working in conjunction with separate positive-valence incentive mechanisms in these downstream circuits remains to be explored.

REFERENCES AND NOTES

1. C. Hull, *Principles of Behavior: An Introduction to Behavior Theory* (D. Appleton-Century Company, New York, 1943).

2. N. E. Miller, *Science* **126**, 1271–1278 (1957).
3. K. Oatley, *Nature* **225**, 797–801 (1970).
4. K. C. Berridge, *Physiol. Behav.* **81**, 179–209 (2004).
5. D. J. Anderson, *Nat. Rev. Neurosci.* **17**, 692–704 (2016).
6. R. C. Bolles, *Theory of Motivation* (Harper & Row, New York, 1967).
7. F. Toates, *Motivational Systems* (Cambridge Univ. Press, Cambridge, 1986).
8. J. Olds, *Science* **127**, 315–324 (1958).
9. J. H. Jennings, G. Rizzi, A. M. Stamatakis, R. L. Ung, G. D. Stuber, *Science* **341**, 1517–1521 (2013).
10. J. N. Betley *et al*., *Nature* **521**, 180–185 (2015).
11. J. H. Jennings *et al*., *Cell* **160**, 516–527 (2015).
12. E. H. Nieh *et al*., *Cell* **160**, 528–541 (2015).
13. Y. Chen, Y. C. Lin, C. A. Zimmerman, R. A. Essner, Z. A. Knight, *eLife* **5**, e18640 (2016).
14. S. M. Sternson, A.-K. Eiselt, *Annu. Rev. Physiol.* **79**, 401–423 (2017).
15. M. L. Mangiapane, T. N. Thrasher, L. C. Keil, J. B. Simpson, W. F. Ganong, *Neuroendocrinology* **37**, 73–77 (1983).
16. R. W. Lind, A. K. Johnson, *J. Neurosci.* **2**, 1043–1051 (1982).
17. M. J. McKinley *et al*., *Physiol. Behav.* **81**, 795–803 (2004).
18. Y. Oka, M. Ye, C. S. Zuker, *Nature* **520**, 349–352 (2015).
19. S. B. G. Abbott, N. L. S. Machado, J. C. Geerling, C. B. Saper, *J. Neurosci.* **36**, 8228–8237 (2016).
20. C. A. Zimmerman *et al*., *Nature* **537**, 680–684 (2016).
21. M. J. McKinley *et al*., *Acta Physiol. (Oxf.)* **214**, 8–32 (2015).
22. M. J. McKinley, D. K. Hards, B. J. Oldfield, *Brain Res.* **653**, 305–314 (1994).
23. L. L. Ji, T. Fleming, M. L. Penny, G. M. Toney, J. T. Cunningham, *Am. J. Physiol. Regul. Integr. Comp. Physiol.* **288**, R311–R321 (2005).
24. C. J. Guenthner, K. Miyamichi, H. H. Yang, H. C. Heller, L. Luo, *Neuron* **78**, 773–784 (2013).
25. *TRAP2* mice were generated by inserting the *2A-iCreERT2* construct into the *Fos* locus via homologous recombination. See the supplementary materials.
26. L. Ye *et al*., *Cell* **165**, 1776–1788 (2016).
27. C. L. Tan *et al*., *Cell* **167**, 47–59.e15 (2016).
28. M. Maruyama *et al*., *Am. J. Physiol. Regul. Integr. Comp. Physiol.* **285**, R1116–R1123 (2003).
29. S. Picelli *et al*., *Nat. Methods* **10**, 1096–1098 (2013).
30. J. T. Fitzsimons, *Physiol. Rev.* **78**, 583–686 (1998).
31. E. L. Sylwestrak, P. Rajasethupathy, M. A. Wright, A. Jaffe, K. Deisseroth, *Cell* **164**, 792–804 (2016).
32. A. Berndt *et al*., *Proc. Natl. Acad. Sci. U.S.A.* **113**, 822–829 (2016).
33. E. S. Boyden, F. Zhang, E. Bamberg, G. Nagel, K. Deisseroth, *Nat. Neurosci.* **8**, 1263–1268 (2005).
34. P. H. Janak, K. M. Tye, *Nature* **517**, 284–292 (2015).
35. P. J. Davern, *Front. Physiol.* **5**, 436 (2014).
36. S. D. Stocker, G. M. Toney, *J. Physiol.* **568**, 599–615 (2005).
37. S. L. Hochstenbach, J. Ciriello, *Brain Res.* **713**, 17–28 (1996).
38. T.-W. Chen *et al*., *Nature* **499**, 295–300 (2013).
39. L. A. Gunaydin *et al*., *Cell* **157**, 1535–1551 (2014).
40. L. DeNardo, L. Luo, *Curr. Opin. Neurobiol.* **45**, 121–129 (2017).

ACKNOWLEDGMENTS

We thank C. Manalac and N. Pichamoorthy for mouse genotyping, M. Lovett-Barron and E. Richman for initial experimental assistance, J. Ren and T. Davidson for fiber photometry rig construction, C. Guenthner for *TRAP2* construct design and cloning, X. Wang and E. Sylwestrak for smFISH advice, L. Ye for CLARITY advice, and A. Chen for FACS assistance. We are grateful to members of the K.D. and L.L. laboratories for providing comments and advice throughout the project and E. Richman, E. Scheer, C. Guenthner, D. Friedmann, M. Lovett-Barron, F. Gore, A. Shuster, S. Lomvardas, and T. Bonhoeffer for comments on the manuscript. W.E.A. is supported by a Fannie & John Hertz Foundation Fellowship and an NSF Graduate Research Fellowship. K.M.L. is a Siebel Investigator in the Stanford University School of Medicine. K.D. is supported by the Defense Advanced Research Projects Agency Neuro-FAST program, the NOMIS Foundation, the Tarlton Foundation, the Wiegers Family Fund, the Nancy and James Grosfeld Foundation, the H. L. Snyder Medical Foundation, and the Samuel and Betsy Reeves Fund. K.D. and L.L. are investigators of the Howard Hughes Medical Institute. This work was supported by a Hughes Collaborative Innovation Award and by National Institute of Mental Health and NSF grants (to L.L. and K.D.). All primary histological, physiological, and behavioral data are archived in the Departments of Biology and Bioengineering, Stanford University, and all optogenetic tools are freely available upon request (www.optogenetics.org). RNA-sequencing data are deposited at Gene Expression Omnibus: GSE101487.

SUPPLEMENTARY MATERIALS

www.sciencemag.org/content/357/6356/1149/suppl/DC1
Materials and Methods
Figs. S1 to S9
Table S1
Movie S1
References (*41*–*55*)

16 May 2017; accepted 26 July 2017
10.1126/science.aan6747

Thirst-associated preoptic neurons encode an aversive motivational drive

William E. Allen, Laura A. DeNardo, Michael Z. Chen, Cindy D. Liu, Kyle M. Loh, Lief E. Fenno, Charu Ramakrishnan, Karl Deisseroth and Liqun Luo

Science **357** (6356), 1149-1155.
DOI: 10.1126/science.aan6747

Thirst-quenching neural mechanisms

To maintain homeostasis, physiological imbalances produce motivational drives. Thirst is one of the strongest drives. Allen *et al.* identified a distinct population of neurons in a brain region called the median preoptic nucleus that are activated during thirst (see the Perspective by Gizowski and Bourque). The activity of these neurons integrates the recent history of water intake and adaptively regulates goal-directed behavior. When thirsty, animals consume water, which in turn reduces the aversive activity of the neurons. This action is repeated until the level of aversion falls below the threshold necessary to evoke this behavior.

Science, this issue p. 1149; see also p. 1092